Exposure of Man in the Near-Field of a Resonant Dipole: Comparison Between Theory and Measurements

MARIA A. STUCHLY, SENIOR MEMBER, IEEE, RONALD J. SPIEGEL, MEMBER, IEEE, STANISLAW S. STUCHLY, SENIOR MEMBER, IEEE, AND ANDRZEJ KRASZEWSKI

Abstract—**The rate of the radio frequency energy deposition in a block model of the human body exposed in the near-field of a resonant dipole at 350 MHz was calculated using the moment method. Detailed maps of the electric field strength in a homogeneous model of a realistic shape under the same exposure conditions were obtained using a computer-controlled scanning system and an implantable electric field probe. A comparison of the measurement data with the calculations shows a relatively good agreement when average values over relatively large volumes are concerned; however, the calculations do not show large spatial gradients and tend to underestimate the magnitude of "hot spots" observed experimentally.**

I. Introduction

RECENT PROGRESS in telecommmunications technology and applications has resulted in widespread and continuously growing use of portable and mobile radio transmitters. One aspect of these developments is the resulting exposure to radio frequency fields, and consequently, a need to assess the safety of the device user.

The dose rate, or the rate at which radio frequency (RF) electromagnetic energy is imparted into the body, defined as the specific absorption rate (SAR), is used in quantifying biological effects and formulating standards on exposure to RF fields [1], [2]. It is also recognized that the spatial distribution of the SAR within the exposed body, and in some interactions also other parameters play an essential role [3].

Numerical methods have been developed to calculate the SAR distribution in very simplified block models of man [4]–[6], and in a more realistic model [7], both in the far-field. The more realistic model has also been employed for evaluation of the SAR distribution in the near-field, when there is no coupling between the radiation source and the irradiated object [8]. Several recent reviews have summarized the computational methods [9]–[11].

Manuscript received February 19, 1985; revised August 26, 1985. This work was supported in part by grants from the U.S. Office of Naval Research, Health and Welfare Canada and the Natural Sciences and Engineering Research Council of Canada.

M. A. Stuchly is with the Radiation Protection Bureau, Health and Welfare Canada, Ottawa, Ont. K1A OL2.

R. J. Spiegel is with the U.S. Environmental Protection Agency, Health Effects Research Laboratory, Research Triangle Park, NC 27711.

S S. Stuchly and A. Kraszewski are with the Department of Electrical Engineering, University of Ottawa, Ont. K1N 6N5.

IEEE Log Number 8405924

The SAR distribution can also be determined experimentally, usually in scaled-down models of man by thermography [12], or by implantable electric field probes.

Because of the geometrical and electrical complexity of the human body, the spatial distribution of the SAR resulting from exposures in the near-field of antennas, as in the case for portable transmitters, is difficult to determine by analytical or experimental methods. The tensor integral method has been used to calculate the SAR distribution in a block model of man consisting of 180 cells exposed to a resonant dipole in the near-field with mutual coupling between the antenna and body due to their close proximity [13], [14]. A computer-controlled measurement system and implantable electric field probes were utilized in obtaining detailed maps of the SAR in a full-scale model of the human body [15], [16].

In this paper, we present the calculations and measurements of the spatial distribution and average SAR's for various body parts for a full-scale model of man exposed in the near-field of a resonant dipole at 350 MHz. The frequency of 350 MHz was selected because of the previously reported resonance of the head [17], and because it is relatively close to the frequencies used in FM portable/mobile radios (403–430 MHz). The results obtained by the two methods are compared, and limitations and advantages of both methods are outlined.

II. Calculations

The electric fields and, therefore, the SAR distribution inside a model of the human body near a dipole antenna are calculated by the tensor integral method described in detail in [13] and briefly in [14]. The human block model consists of 180 cubical cells of varying sizes arranged to best fit the contour of a 70-kg man [7]. Because of body symmetry, only the values within one half of the body are presented. A thin resonant dipole is located close to the head in a location whose coordinates are given in Table I. Other essential exposure and model parameters are also summarized in Table I.

III. Measurements

The electric field intensity was measured, and the SAR subsequently calculated in more than 650 locations within half of the model of the human body. An implantable

0018-9480/86/0100-0026$01.00 ©1986 IEEE

TABLE I
ESSENTIAL MODEL AND EXPOSURE PARAMETERS

Parameter	Calculations	Experiment
Frequency	350 MHz	350 MHz
Actual dipole length	0.5 λ	0.43 λ
Dipole length/radius	200	117
Input impedance	48.3 Ω	50 Ω
Distance from the body	7.3 cm	8 cm
Distance dipole axis/head top (vertically)	34.8 cm	38 cm
Model height	170 cm	175 cm
Dielectric constant	37	37
Conductivity	0.95 S/m	0.95 S/m

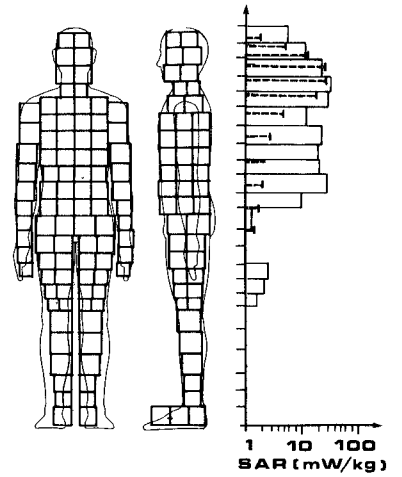

Fig. 1. Comparison of the specific absorption rate (SAR) calculated and measured along a selected axis shown by vertical dashed lines. Blocks represent the calculated values, while the measured values are depicted by horizontal dashed lines, for $f = 350$ MHz, 1-W input power to the antenna, E polarization, and for the location of the dipole given in Table I.

isotropic electric field probe (EIT) model 979 (manufactured by Electronic Instrumentation and Technology, Inc.) was used. The probe was fully evaluated and calibrated prior to the experiment [18] and the calibration was spot checked during the measurements. The computer-controlled scanning system [15], [16] performed a set of measurements at 650 locations in less than 1.5 h. The repeatability of the SAR measurements was better than ± 0.5 dB, as tested on up to 15 repetitions under various power levels and on various days. The uncertainty of the SAR determination was estimated to be approximately ± 1 dB. The main contribution to the SAR measurement uncertainty was due to the limitations of performance of the electric field probe and its calibration [18]. Each data point presented in this paper is an average of four to five measurements.

A full-scale model of an anatomically proportional average man (175 cm, 70 kg, based on a plastic model Remcal, manufactured by Alderson Research Lab. Inc.) was made of low-density Styrofoam sheets 2.5 cm thick, which were glued together. The model was positioned horizontally (face up) in an anechoic chamber (dimensions $4.6 \times 3 \times 2.1$ m). The antenna was placed under the model, and the electric field probe was immersed in the model from its top. The distance between the chamber floor, which was covered with RF absorber, and the antenna was 60 cm (from the absorber); the distance between the mold and the chamber walls and ceiling was 1.5 m or more. The reflections from the chamber walls, floor, and ceiling were measured, and were found to be below -20 dB at a frequency of 350 MHz.

The mold was partly open in the torso area, and holes large enough for inserting the probe were drilled in other locations, more details about the mold are given elsewhere [16]. The mold was filled with a low-viscosity (to facilitate probe immersion) mixture having average tissue properties (2/3 muscle tissue) at a frequency of 350 MHz (Table I). Essential model and exposure parameters are given in Table I. The resonant dipole was shortened to 0.43 λ, to achieve matching to a 50-Ω transmission line. The dipole input VSWR was less than 1.2 with the model of man placed at a distance of 8 cm.

IV. RESULTS AND DISCUSSION

The measured local values of the SAR in the center cross section of the model (dashed lines) are compared with the calculated SAR values in the corresponding cells (solid-line bars), as illustrated in Fig. 1. The contours of the two models were matched along the main axis of the body. A small difference (less than 3 percent) in the height of the two models (see Table I) resulted mainly from the curvature of the head. When the measured location was on the border of two cells or very close to it, the average SAR for the two cells was utilized for the comparison. Both the calculated and the measured SAR values were normalized to 1-W input power to the dipole. It can by seen that the theoretical and measured SAR's in the neck region in the center of the body are in reasonably good agreement. However, overall, the spatial distribution of the SAR predicted by the calculation is significantly different from the measured values, with differences of an order of magnitude at some locations (notice the logarithmic scale). This may be an unfair comparison, as the local values of the SAR within spheres of a diameter of 0.9 cm (the probe diameter) are compared with the average values in cubes of approximately 7 cm (the average cell size). In the comparisons that follow, the calculated values are compared with the measured values averaged over certain volumes.

Fig. 2 shows a comparison the the spatially averaged calculated and measured SAR's along two selected body axes. The SAR values are, in both cases, averaged over the tissue volume contained between the body surfaces in the direction of the wave propagation. This means that the values are the averages over two or three cells, except in the legs, for the calculated SAR's, and the averages over the

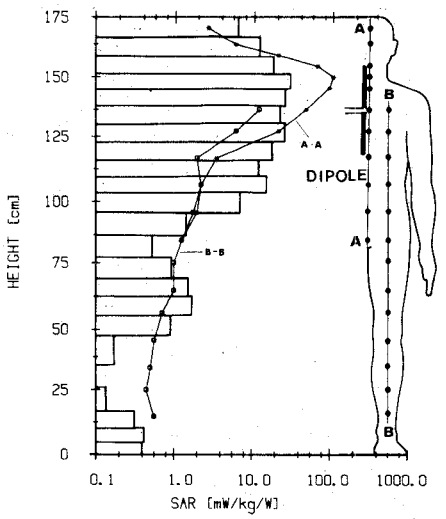

Fig. 2. Comparison of the calculated and measured specific absorption rate (SAR) averaged along the direction of the wave propagation (perpendicular to the axis of the body). The blocks show the calculated values averaged over the cells in the direction of wave propagation, and the points represent the measured data averaged over cylinders 0.9 cm in diameter, for $f = 350$ MHz, 1-W input power to the antenna, E polarization, and for the location of the dipole given in Table I.

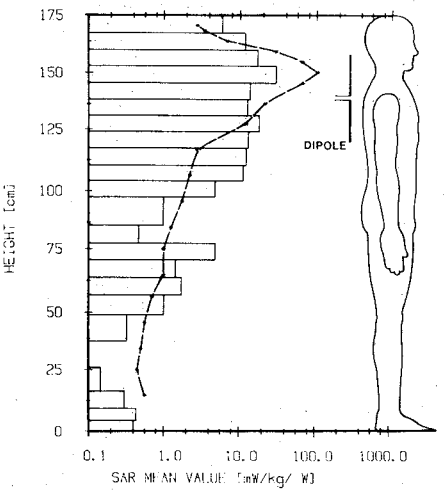

Fig. 3. Comparison of the specific absorption rate (SAR) averaged over horizontal tissue slabs. The blocks show the calculated values, and the points the measured data, for $f = 350$ MHz, 1-W input power to the antenna, E polarization, and for the location of the dipole given in Table I.

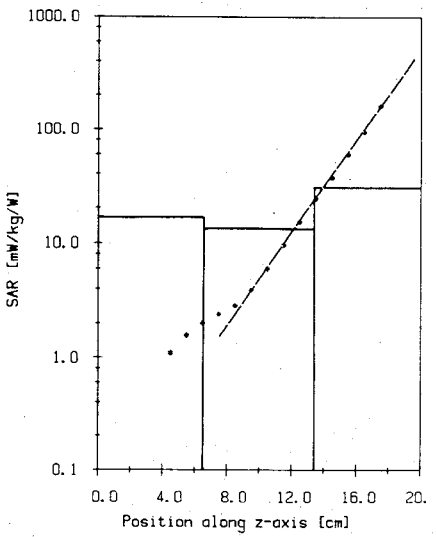

Fig. 4. The specific absorption rate (SAR) on the dipole axis in the torso. The blocks show the calculated values, the points the measured data, the straight line shows the least-square fit into data points for $z \geq 8$ cm of the curve $\mathrm{SAR} = A\exp(-\alpha z)$. The body surface at which the wave is incident is at $z = 20$ cm, and the wave propagates toward $z = 0$, with $f = 350$ MHz, 1-W input power to the antenna, E polarization, and for the location of the dipole given in Table I.

cylindrical volume of 0.9-cm diameter for the measured SAR's. Since the probe did not penetrate to the very bottom of the back surface of the mold appropriate curves (exponential) were fitted to the measurement points using the least-square method to calculate SAR's at the model surface. These data points together with the measured SAR values were used to calculate the average SAR's.

The general shape of both spatial distributions looks similar. It is clear that the theory does not predict to the same extent an increase in the SAR in the neck region. However, the largest differences between the predicted and measured values are about 5 to 6 times rather than 10, as it was for the previous comparison (see Fig. 1).

A much better agreement between the theory and the experiment can be seen in the SAR values averaged over the horizontal tissue layers presented in Fig. 3. The arms are not included in these averages. The calculations in this case underestimate the maximum SAR in the neck by a factor of three.

The whole-body average SAR's calculated and measured are 7.9 and 6.3 ± 1.2 mW/kg, respectively. The difference is within the uncertainty of measurements (because of the extrapolation involved the accuracy of the whole-body average estimated at ± 25 percent is much worse than that of the local SAR's) and can be attributed to the difference in the distance between the dipole and the body in the calculations and experiment (7.3 versus 8 cm). As an example of regional SAR differences, the head/neck area calculated average SAR is 17 mW/kg, while the measured value is 28 mW/kg. The difference in this case is relatively large but consistent with previously noted differences in the spatial distribution of the SAR. The SAR in the neck is extremely sensitive to the shape of the neck.

A very important feature of the RF energy deposition in the human body in the near-field of radiators at 350 MHz, which is not evident from the analysis of the block model of man, is illustrated in Fig. 4. This figure shows the SAR in the torso on the center point of the dipole along the direction of the wave propagation. The dipole center point is located at 38 cm from the head top. The wave is incident at the torso wall at $z = 20$ cm and the torso extends to approximately $z = 0$. The vertical columns show the calculated SAR in the three body cells, the points show the experimental data. The dashed line represents a least-square fit of an exponential relationship

$$\mathrm{SAR} = A\exp(-\alpha z). \tag{1}$$

Two important observations can be made. Firstly, at a frequency of 350 MHz, the SAR decreases exponentially in

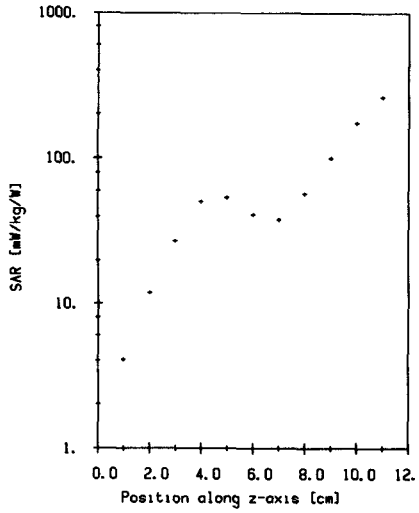

Fig. 5. The specific absorption rate (SAR) in the neck. The points show the measured data at the height 150 cm from the feet base, the neck surface at which the wave is incident is at $z = 12$ cm, and the wave propagates toward $z = 0$, with $f = 350$ MHz, 1-W input power to the antenna, E polarization, and for the location of the dipole given in Table I.

the torso within about one-half of the torso width. Beyond that point the SAR values are very low, more than 100 times below those on the surface. Furthermore, the attenuation coefficient $\alpha = 0.46 \pm 0.01$ is, within the fitting error, equal to that calculated for the planar model with electrical properties of the tissue simulating material, $\alpha = 0.49 \pm 0.02$. Secondly, the theory does not show the decrease of the SAR with distance away from the plane of the incident wavefront. It is apparent from Fig. 4, that the average SAR's for the layers of about 7 cm corresponding to the cells' width are significantly different, particularly for the two outer cells. The exponential decay in the SAR is typical for other locations along the torso and the head. Only in the center of the neck, 150 cm from the feet base, can an increase in the SAR close to the neck center be observed (Fig. 5). The SAR close to the neck center is approximately 50 mW/kg, as compared with 440 mW/kg at the neck surface and the average SAR of 115 mW/kg for the cylinder of 0.9 cm in diameter on the neck axis between the neck surface of the wave incidence and the opposite surface.

Our results are to a certain extent different from the previously reported agreement between the calculated and measured SAR distributions [4]–[6]. However, the comparisons were done for much simpler shapes and different exposure conditions. The reported agreement is even more impressive in view of a relatively simple electric field probe that was used for the measurements reported in [4] and [6]. On the other hand, for more realistic models, for some regions such as the neck, differences of the order of 10 to 20 between the calculated and measured values of the SAR were previously reported [7].

We feel that the differences between the calculated and the measured values of the SAR are due to the limitations of the calculations because the accuracy of the measurements was verified using simple geometrical bodies [19]. Although it was stipulated that the analysis of the block model of man can be used up to 500 MHz [4]–[7], the limits on the cell size were suggested [20]. The cell size used in our calculations is greater than the suggested limit [20]. Furthermore, other deficiencies of the numerical analysis using the cubical block model of man in calculating the SAR distribution have recently been suggested [21]. These, however, have also been questioned [22].

V. Conclusions

The specific absorption rate (SAR) averaged over various body volumes and the spatial distributions of the SAR calculated and measured were compared for the near-field exposure by a resonant dipole at 350 MHz. The calculations were performed using the method of moments to solve the tensor integral equations for a block model of man consisting of total of 180 cubical cells. A computer-controlled scanning system and an implantable electric field probe were used to measure local values of the SAR in 650 locations within half of the model of a human body with an uncertainly of approximately ± 1 dB.

The whole-body average SAR's obtained by both methods are in good agreement. The values of the SAR averaged over smaller volumes and the spatial distribution of the SAR are different by factors ranging from 3 to 10. The theoretical analysis does not predict an exponential decrease in the SAR values in the direction of the wave propagation away from the surface upon which the wave is incident. Relatively large spatial gradients of the SAR are similarly not apparent from the calculations.

The main limitations of the calculations result from a relatively small number of blocks and the resulting relatively large size of the blocks as compared to the wavelength in the tissue [20]. Furthermore, limited accuracy is inherent in the method employed [21]. Differences in the shapes of the models may play some role, but probably less significant than the other factors. The neck may be considered as the region where shape differences have been sufficiently large so as to affect the SAR.

In view of the computational difficulties in extending the available theoretical methods to more refined realistic models of the human body, at present experimental methods appears to be a viable alternative for determination of the spatial distribution of the SAR in models of humans exposed in the near-field of radio frequency antennas.

References

[1] "Radiofrequency electromagnetic fields; properties, quantities and units, biophysical interactions and measurements," NCRP Rep. No. 67, 1981.

[2] "Safety levels with respect to human exposure to radio frequency electromagnetic fields, 300 kHz to 100 GHz," ANSI C95.1-1982.

[3] W. R. Adey, "Tissue interactions with non-ionizing electromagnetic fields," *Phys. Rev.*, vol. 61, pp. 435–513, 1981.

[4] B. S. Guru and K. M. Chen, "Experimental and theoretical studies on electromagnetic fields induced inside finite biological bodies," *IEEE Trans. Microwave Theory Tech.*, vol. MTT-24, pp. 433–440, 1976.

[5] K. M. Chen and B. S. Guru, "Induced electromagnetic field and absorbed power density inside human torso," *IEEE Trans. Microwave Theory Tech.*, vol. MTT-24, pp. 1450–1453, 1976.

[6] K. M. Chen and B. S. Guru, "Internal EM field and absorbed

power density in human torso induced by 1–500 MHz EM waves," *IEEE Trans. Microwave Theory Tech.*, vol. MTT-25, pp. 746–756, 1977.
[7] M. J. Hagmann, O. P. Gandhi, and C. H. Durney, "Numerical calculation of electromagnetic energy deposition for a realistic model of man," *IEEE Trans. Microwave Theory Tech.*, vol. MTT-27, pp. 804–809, 1979.
[8] I. Chatterjee, M. J. Hagmann, and O. P. Gandhi, "Electromagnetic energy deposition in an inhomogeneous block model of man for near-field irradiation conditions," *IEEE Trans. Microwave Theory Tech.*, vol. MTT-288, pp. 1452–1459, 1980.
[9] R. J. Spiegel, "A review of numerical models for predicting the energy deposition and resultant thermal response of humans exposed to electromagnetic fields," *IEEE Trans. Microwave Theory Tech.*, vol. MTT-32, pp. 730–746, 1984.
[10] C. H. Durney, "Electromagnetic dosimetry for models of humans and animals: A review of theoretical numerical techniques," *Proc. IEEE*, vol. 68, pp. 33–40, 1980.
[11] O. P. Gandhi, "Electromagnetic absorption in an inhomogeneous model of man in realistic exposure conditions," *Bioelectromagn.*, vol. 3, pp. 81–90, 1982.
[12] A. W. Guy, "Analysis of electromagnetic fields induced in biological tissues by thermographic studies in equivalent phantom models," *IEEE Trans. Microwave Theory Tech.*, vol. MTT-19, pp. 205–214, 1971.
[13] K. Karimullah, K. M. Chen, and D. P. Nyquist, "Electromagnetic coupling between a thin-wire antenna and a neighboring biological body: Theory and experiment," *IEEE Trans. Microwave Theory Tech.*, vol. MTT-28, pp. 1218–1225, 1980.
[14] R. J. Spiegel, "The thermal response of a human in the near-zone of a resonant thin-wire antenna," *IEEE Trans. Microwave Theory Tech.*, vol. MTT-30, pp. 177–185, 1982.
[15] S. S. Stuchly, M. Barski, B. Tam, G. Hartsgrove, and S. Symons, "A computer-based scanning system for electromagnetic dosimetry," *Rev. Sci. Instrum.*, vol. 54, pp. 1547–1550, 1983.
[16] A. Kraszewski, M. A. Stuchly, S. S. Stuchly, G. Hartsgrove, and D. Adamski, "Specific absorption rate distribution in a full-scale model of man at 350 MHz," *IEEE Trans. Microwave Theory Tech.*, vol. MTT-32, pp. 779–783, 1984.
[17] M. J. Hagmann, O. P. Gandhi, J. A. D'Andrea, and I. Chatterjee, "Head resonance: Numerical solutions and experimental results," *IEEE Trans. Microwave Theory Tech.*, vol. MTT-27, pp. 809–813, 1979.
[18] M. A. Stuchly, A. Kraszewski, and S. S. Stuchly, "Implantable electric field probes—Some performance characteristics," *IEEE Trans. Biomed. Eng.*, vol. BME-31, pp. 526–530, 1984.
[19] C. H. Wong, S. S. Stuchly, A. Kraszewski, and M. A. Stuchly, "Probing electromagnetic fields in lossy spheres and cylinders," *IEEE Trans. Microwave Theory Tech.*, vol. MTT-32, pp. 824–828, 1984.
[20] M. J. Hagmann, O. P. Gandhi, and C. H. Durney, "Upper bound on cell size for moment-method solutions," *IEEE Trans. Microwave Theory Tech.*, vol. MTT-25, pp. 831–832, 1977.
[21] H. Massoudi, C. H. Durney, and M. F. Iskander, "Limitations of the cubical block model of man in calculating SAR distributions," *IEEE Trans. Microwave Theory Tech.*, vol. MTT-32, pp. 746–751, 1984.
[22] M. J. Hagmann, "Comments on 'Limitations on the cubical block model of man in calculating SAR distributions,'" *IEEE Trans. Microwave Theory Tech.*, vol. MTT-33, pp. 347–350, 1985.

Maria A. Stuchly (M'71–SM'76) received the M.S. and Ph.D. degrees in electrical engineering from Warsaw Technical University and Polish Academy of Sciences in 1962 and 1970, respectively.

From 1962 to 1970, she was employed as a senior R&D engineer in a subsidiary of the Polish Academy of Sciences in Warsaw, Poland. Between 1970 and 1976, she was engaged in research in the field of microwave instrumentation and measurements, and microwave power applications at the Departments of Electrical Engineering and Food Science at the University of Manitoba. Since 1976, she has been with the Non-Ionizing Radiation Section, Radiation Protection Bureau, Health and Welfare Canada, where she is responsible for the development of microwave radiation protection standards and carries out research in the field of microwave radiation. Since 1978, she has been nonresident professor of Electrical Engineering at the University of Ottawa.

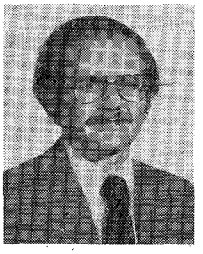

Ronald J. Spiegel was born in Cleveland, OH. He received the B.E.E. degree in 1964 from the Georgia Institute of Technology, and the Ph.D. degree in electrical engineering in 1970 from the University of Arizona.

Form 1971 to 1972, he was a Post-Doctoral Fellow in biomedical engineering at Duke University. In 1973, he joined the Boeing Aerospace Company, Seattle, WA, as a research engineer engaged in studies of nuclear electromagnetic pulse (EMP) effects on aeronautical electrical systems. From 1974 to 1976, he was with IIT Research Institute, Chicago, IL, involved in research in bioelectromagnetics and extra-low-frequency (ELF) coupling, interference mitigation, and environmental studies associated with the Navy Seafarer antenna. From 1976 to 1980, he was with Southwest Research Institute, San Antonio, TX, performing research in a variety of areas such as EMC, electrostatics, bioelectromagnetics, and electromagnetic geophysical exploration. He is presently with the U.S. Environmental Protection Agency, Research Triangle Park, NC, and is Chief of the Biological Engineering Branch. His current research efforts are concentrated in the area of microwave field interaction with biological media and dosimetric methods.

Dr. Spiegel is a member of the Eta Kappa Nu, Sigma Xi, Bioelectromagnetics Society, and is a Registered Professional Engineer.

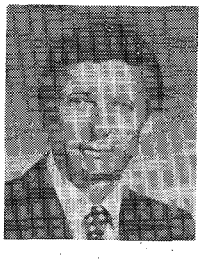

Stanislaw S. Stuchly (M'70–SM'72) was born in Lwow, Poland, on November 20, 1931. He received the B.Sc. degree from the Technical University, Gliwice, Poland, and the M.Sc. from the Warsaw Technical University, both in electrical engineering, in 1953 and 1958, respectively, and the Ph.D. degree from the Polish Academy of Sciences, Warsaw, Poland, 1968.

From 1953 to 1959, he was a research engineer in the Industrial Institute for Telecommunications, Warsaw, Poland, engaged in research in the field of radar and microwave theory and techniques. From 1959 to 1963, he was with the Warsaw Technical University as an Assistant Professor working in the field of microwave measurements. In 1963, he joined UNIPAN — Scientific Instruments, Subsidiary of the Polish Academy of Sciences as a manager of the Microwave Instruments Division. In 1970, he immigrated to Canada. From 1970 to 1976, he was with the University of Manitoba, Winnipeg, Canada, as an Associate Professor in the Department of Agricultural Engineering and Electrical Engineering.

Since 1977, he has been with the Department of Electrical Engineering, University of Ottawa, Canada, where he is presently a professor and teaches courses and carries out research in the field of microwave theory and techniques, as well as digital instrumentation and applications of computers. He is also a nonresident professor at Carleton University in Ottawa.

He is the author of over 80 scientific papers in the field of microwave theory and techniques, as well as analog and digital instrumentation and holds 18 patents.

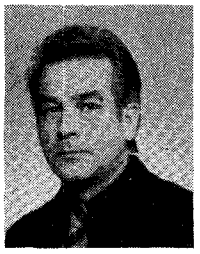

Andrzej Kraszewski was born in Poznan, Poland, on April 22, 1933. He received the M.Sc. degree in electrical engineering from the Technical University of Warsaw, Poland, in 1958 and the D.Sc. degree in technical sciences from the Polish Academy of Sciences, (PAN), Warsaw, in 1973.

In 1953, he joined the Telecommunication Institute, Warsaw, Poland, in research and development of microwave components and systems. In 1963, he joined UNIPAN Scientific Instruments, subsidiary of the Polish Academy of Sciences, as the Head of the Microwave Laboratory. In 1972, he became the Manager of the Microwave Department of WILMER Instruments and Measurements, a subsidiary of the Polish Academy of Sciences in Warsaw, where he codeveloped microwave instruments for moisture content measurements and control. Since November 1980, he has been a visiting professor at the University of Ottawa, Ottawa, Canada, where he is engaged in research of interactions between dielectrics and electromagnetic fields. He is the author of several books on microwave theory and techniques, has published more than 80 technical papers on the subject, and holds 18 patents.

Dr. Kraszewski is a member of the International Microwave Power Institute, the Polish Electricians Association and is a member of the Editorial Board of the *Journal of Microwave Power*. He has received several professional awards, among them the State Prize in Science, in 1980.